Journal of Alloys and Compounds 507 (2010) 341–344

Contents lists available at ScienceDirect

Journal of Alloys and Compounds

journal homepage: www.elsevier.com/locate/jallcom

Electronic structure and visible-light-driven photocatalytic performance of Cd_2SnO_4

Xianli Huang [a,b], Jun Lv [a], Zhaosheng Li [a], Zhigang Zou [a,*]

[a] Eco-Materials and Renewable Energy Research Center (ERERC), National Laboratory of Solid State Microstructure, Department of Physics, Nanjing University, Nanjing 210093, China
[b] Department of Applied Chemistry, Nanjing University of Astronautics and Aeronautics, Nanjing 210016, China

ARTICLE INFO

Article history:
Received 25 November 2009
Received in revised form 18 May 2010
Accepted 28 May 2010
Available online 8 June 2010

Keywords:
Semiconductor
Band structure
Photocatalysis
Oxide

ABSTRACT

Cd_2SnO_4 conducting oxide was prepared via a solid state reaction method, and its photocatalytic O_2 evolution performance was presented. The band gaps were estimated to be 2.3 eV for Cd_2SnO_4 calcined at 1050 °C, 2.4 eV for Cd_2SnO_4 calcined at 900 °C and 800 °C. The catalysts prepared at 800 °C possessed the largest surface area and the best catalytic activities. The band structure was calculated by a density function theory method. The conduction band bottom was composed of Cd5s, Sn5s and Sn5p orbits, and the valence band top of Cd4d and O2p. The high photocatalytic activities of Cd_2SnO_4 were attributed to its specific band structures.

1. Introduction

Photocatalytic hydrogen production has attracted more and more attentions due to the increasing energetic and environmental pressure in recent years. Many oxide photocatalysts are developed for the photocatalytic water-splitting process, including TiO_2, $BaTi_4O_9$, $K_2La_2Ti_3O_{10}$, $NaTaO_3$, etc. [1–3]. Despite of their high efficiencies, these photocatalysts could only be utilized in the UV region, whose energy sum up to only 4% of total solar energy. Furthermore, it has been revealed that the bottom of conducting band of oxides is not negative enough for H_2 reduction potentials, thus possibly able to be used as catalysts for O_2 evolution, but unable to be used as photocatalysts for direct water splitting into hydrogen and oxygen [4].

However, two-photon processes (Z-scheme) have been demonstrated to be an efficient way to achieve the overall water splitting [5–7]. In a typical Z-scheme, the hydrogen-evolving and the oxygen-evolving catalysts, together with the redox shuttle, cooperate to form a reducing and oxidizing reactions recycle. For instance, Pt-loaded Cr and Ta co-doped $SrTiO_3/WO_3$, and Pt-loaded $TaON/WO_3$ systems were showed to be able to produce H_2 and O_2 simultaneously in a stoichiometric ratio, in which I^-/IO_3^- or Fe^{2+}/Fe^{3+} was used as redox couples [5–7]. In order to design and manufacture the Z-scheme systems, highly active visible-light-driven photocatalysts for hydrogen or oxygen evolution are all indispensable.

Up to now, there are still very few highly efficient catalysts, except for WO_3 and $BiVO_4$ [8,9]. In a view of band structures, the visible-light absorption of those oxides was realized by overlapping O2p orbit with the V3d, W5d, or Ag5 s orbits. Actually, the 4d-orbit of Cd other than the Ag4d orbit is another candidate for adjusting the top of valence band. In this letter, we present a novel photocatalyst Cd_2SnO_4 with a visible-light response. Cd_2SnO_4 together with its nominal solid solutions $Cd_{1+x}In_{2-2x}Sn_xO_4$ $(0 < x < 0.75)$ is a conducting oxide, and have been widely investigated in a form of bulk ceramics and films [10–12]. But few works were reported concerning its photocatalytic performances. Therefore, here we reported the band structures and photocatalytic properties of oxygen evolution in an $AgNO_3$ aqueous solution.

2. Experimental

All agents, such as SnO_2 (99.5%, Shanghai Agent Co.) and CdO (99.0%, Shanghai Agent Co.) were used as bought. Cd_2SnO_4 was prepared using a solid state reaction method. 5% excess of CdO was used to evade the volatilization of Cd. Stoichiometric SnO_2 and CdO (5% excess) were mixed and milled in an agate mortar, and the mixtures were calcined in an Al_2O_3 crucible at from 1023 K to 1323 K for 6 h.

The phases were identified by powder X-ray diffraction (XRD) method with Cu Kα radiation (Rigaku D/Max-IIIB diffractometer). The specific surface area of the oxide was determined by BET measurement (Micromeritics-2360, Shimadzu, Japan) of nitrogen adsorption at 77 K. The UV–vis diffuse reflectance spectra were measured with UV–vis spectrophotometer (Shimadzu UV-2500), and transformed from reflectance to absorbance by the Kubelka–Munk transformation method.

0.3 g catalyst powder was dispersed into an aqueous $AgNO_3$ solution (5 mmol/L). Before photocatalytic reaction, the closed system was evacuated to get rid of oxygen

---

* Corresponding author. Tel.: +86 025 83686630; fax: +86 025 83686632.
E-mail address: zgzou@nju.edu.cn (Z. Z.ou).

0925-8388/$ – see front matter © 2010 Elsevier B.V. All rights reserved.
doi:10.1016/j.jallcom.2010.05.126

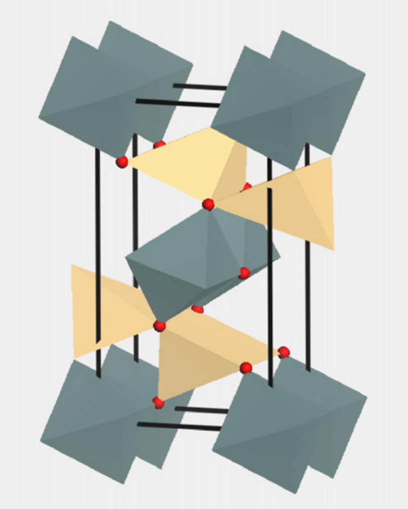

Fig. 1. Unit cell of Cd_2SnO_4.

and nitrogen and filled with Ar gas to 30 torr. The photocatalytic O_2 evolution experiments were carried out under the irradiation of a 300 W Xe lamp with a 420 nm cut-off filter. The amount of evolved O_2 was measured by a GC analyzer (Shimadzu Co., GC8A) which was connected to the circulation system. The band structure was calculated by a CASTEP package with a GGA potential function [13,14]. During the computation, a 4 × 4 × 4 super-cell was built and the cut-off energy was selected to be 340 eV.

3. Results and discussion

3.1. Microstructure characterization

Cd_2SnO_4 possesses a space group of Pbma (No. 55) and an orthorhombic structure [10]. Fig. 1 was the schematic unit cell of Cd_2SnO_4, in which tetrahedra and octahedra were stacked along the ⟨1 1 1⟩ direction. Cd and Sn occupied the tetrahedra and octahedra, respectively [15].

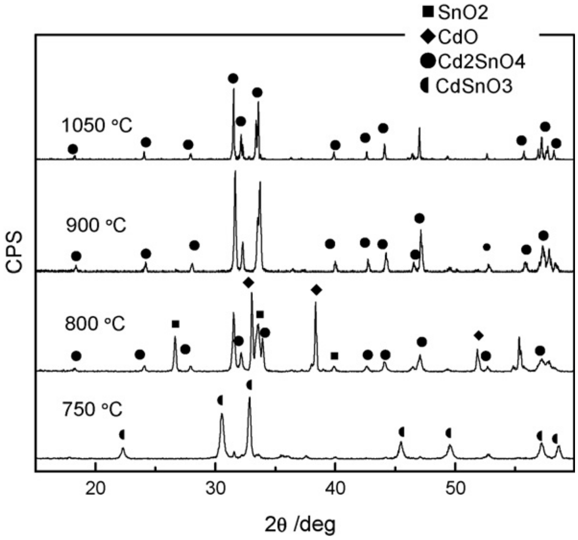

Fig. 2. XRD patterns of Cd_2SnO_4 calcined at different temperatures.

There were mainly two phases in the quasi-binary phase diagram of CdO and SnO_2, i.e., $CdSnO_3$ and Cd_2SnO_4. Fig. 2 showed the XRD patterns of as-purchased CdO and calcined SnO_2 at 750 °C, 800 °C and 1050 °C, respectively. When the calcining temperatures were lower than 800 °C, perovskite $CdSnO_3$ first crystallized, which corresponded well with Ref. [11]. At 800 °C, the resultant was composed mainly of Cd_2SnO_4, and the remnant was of SnO_2 and CdO, which could hardly be eliminated only through elongating calcining duration. When heated at 1050 °C for 6 h, those secondary phases disappeared and single-phased Cd_2SnO_4 was prepared.

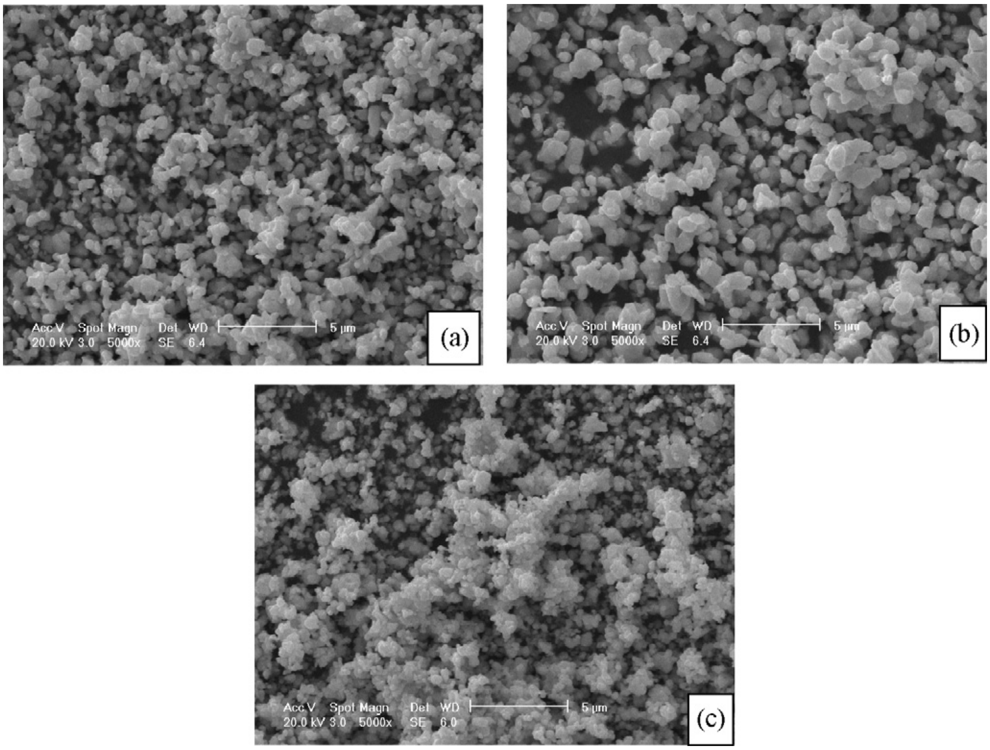

Fig. 3. SEM of Cd_2SnO_4 calcined at different temperatures (a) 800 °C; (b) 900 °C; (c) 1050 °C.

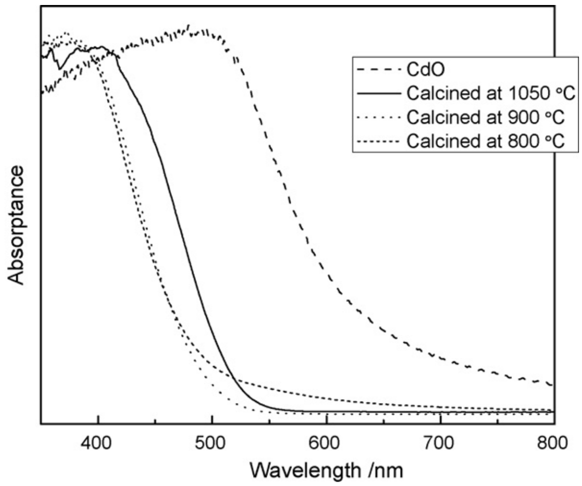

Fig. 4. UV–vis spectra of as-purchased CdO and calcined Cd_2SnO_4 at different temperatures.

According to the Scherrer's formula, the broadening of diffraction peaks between 40° and 50° indicated that the granular size became larger and larger with increasing of calcining temperatures. This fact also corresponded well with the surface areas measurements. The specific surface areas of the Cd_2SnO_4 were 8.76 m^2/g for Cd_2SnO_4 calcined at 800 °C, 6.34 m^2/g for Cd_2SnO_4 calcined at 900 °C and 4.24 m^2/g for Cd_2SnO_4 calcined at 1050 °C.

The SEM photographs of catalysts were shown in Fig. 3. More particles in Fig. 3(c) agglomerated together than those in Fig. 3(a) and (b), which might be the cause of smaller surface areas.

3.2. Photophysical properties

Fig. 4 showed the UV–vis absorption spectra of as-purchased CdO and calcined Cd_2SnO_4 at different temperatures for 6 h. The band gaps of those compounds were estimated by the following formula [16]:

$$\alpha h\nu = A(h\nu - E_g)^n$$

in which α, ν, A, and E_g are absorption coefficient, light frequency, proportionality constant, and band gap, respectively.

The values of n, often taken as a sign of the characteristics of electron transition in semiconductors, was 1.5 for Cd_2SnO_4, indicating the transition in Cd_2SnO_4 was indirectly allowed. The band gaps were, in turn, 2.3 eV for Cd_2SnO_4 calcined at 1050 °C, 2.4 eV for Cd_2SnO_4 calcined at 900 °C and 800 °C, and 2.0 eV for as-purchased CdO. The larger band gaps of Cd_2SnO_4 calcined at 900 °C and 800 °C should be ascribed to the blue-shift induced by relative smaller granular size. The tailing of Cd_2SnO_4 calcined at 800 °C should be derived from the presence of CdO.

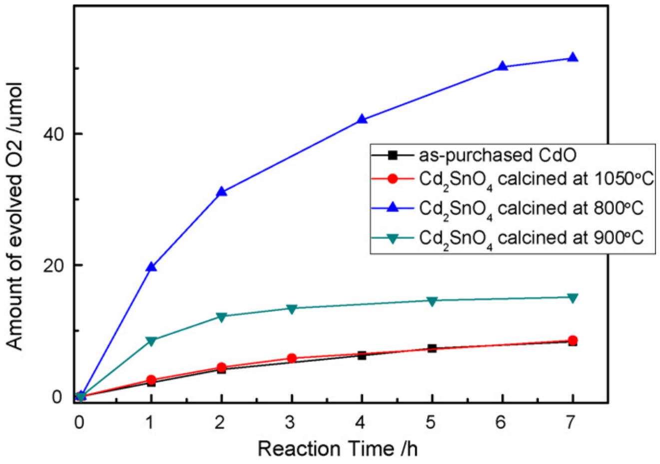

Fig. 5. Amount of evolved O_2 over CdO and calcined Cd_2SnO_4 at different temperatures in the course of irradiation.

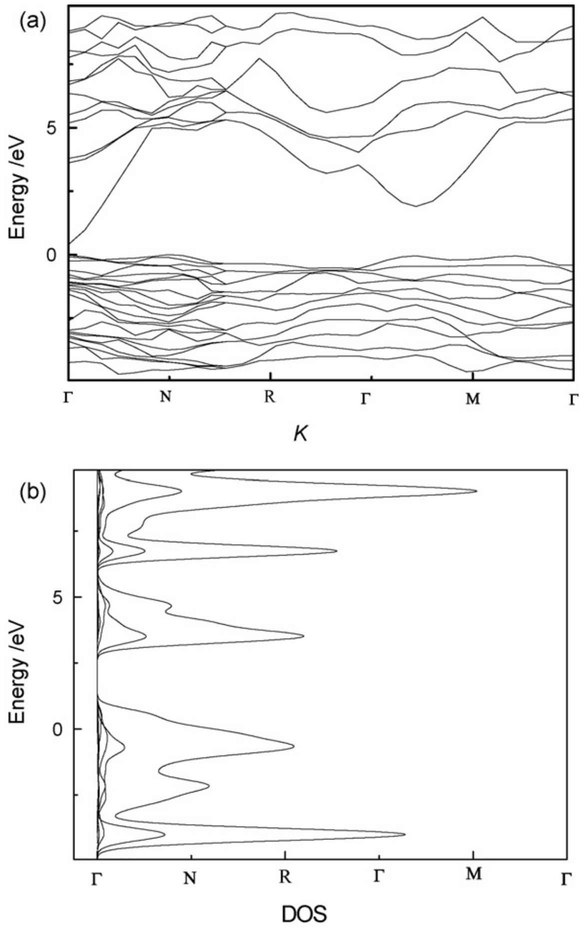

Fig. 6. Band structure (a) and DOS (b) of Cd_2SnO_4.

3.3. Photocatalytic performance of O_2 evolution

Both photocatalytic evolution experiments of O_2 and H_2 were carried out, but no H_2 was evolved over 0.5 wt% Pt-loaded Cd_2SnO_4 after 10 h irradiation in a methanol solution, indicative of that the conduction band bottom was not high enough for H_2 evolution. The photocatalytic experiment results were plotted in Fig. 5. All three catalysts reached to the highest oxygen rate at their first reaction hour, i.e., about 19.6 μmol/h for Cd_2SnO_4 calcined at 800 °C, 8.6 μmol/h for Cd_2SnO_4 calcined at 900 °C, 2.5 μmol/h for Cd_2SnO_4 calcined at 1050 °C. Therefore, Cd_2SnO_4 possessed high visible-light-driven photocatalytic performance and would be a promising candidates materials for building the Z-scheme.

As mentioned above, Cd_2SnO_4 powder calcined at 800 °C was composed of two phases. In order to exclude the influence of CdO, photocatalytic oxygen evolution experiment over CdO was carried out under the same conditions and the experimental results were shown in Fig. 5 as well. Although the as-purchased CdO catalyst possessed a largest specific surface area 12.53 m^2/g, the photocatalytic evolution rate was 2.1 μmol/h. Therefore, the highest activities of Cd_2SnO_4 calcined at 800 °C should not be ascribed to the existence of CdO, but to the larger specific surface areas.

3.4. Band structures

Like many other photocatalysts, the high catalytic performance of Cd_2SnO_4 was closely related to its band structures. The band structure and density of states (DOS) of Cd_2SnO_4 were shown in Fig. 6(a) and (b), respectively. In Fig. 6(a), the valence band maximum and conduction band minimum did no share the same *k* values, indicating that the transition in Cd_2SnO_4 was indirectly allowed. The calculated result agreed well with the results of curve-fitting to the onset in Fig. 4. The DOS in Fig. 6(b) illustrated the composition of the conduction band and the valence band. The conduction band was mainly composed of Cd5s, Sn5s and Sn5p orbits, and the overlapping of Cd4d with O2p pushed up the valence band top and thus Cd_2SnO_4 could absorb visible light.

It was worthy to note that DOS of the conduction band in Fig. 6(a) varied violently with the variation of *k*. The velocity of electron in the *k*-space is proportional to the slope of the DOS, so the photo-excited electrons in the conduction band of Cd_2SnO_4 possessed a large velocity. Such a large velocity could help the photo-excited carriers be separated and transferred easily to the surface of the photocatalysts [17]. This might be to the reason why Cd_2SnO_4 possessed high O_2 evolution activities under the visible-light irradiation.

4. Conclusions

Cd_2SnO_4 was prepared by a solid state reaction method and its photocatalytic oxygen evolution activities under the irradiation of visible light were presented. Cd_2SnO_4 calcined at 800 °C showed good oxygen evolution activities under visible light. The photocatalytic performance was discussed together with its band structures. The experimental and calculation results showed that Cd4d overlapped with O2p brought about a narrowed band gap. The band structure adjustment via overlapping of Cd4d with O2p could be anther feasible way to develop and design oxide photocatalysts working in the visible light.

Acknowledgements

The authors gratefully acknowledge the financial support from the National High Technology Research Project of China (No. 2006AA05Z113), the National Natural Science Foundation of China (No. 20528302), and the Jiangsu Provincial Natural Science Foundation of China (No. BK2006718). One of our authors, Dr. Xianli Huang, would give thanks to the NUAA Research Funding (NO. 2010159). The National Basic Research Program of China (No. 2007CB613305) is also gratefully acknowledged.

References

[1] K. Yamaguti, S. Sato, J. Chem. Soc., Faraday Trans. 81 (1985) 1237–1246.
[2] S. Ikeda, M. Hara, J.N. Kondo, K. Domen, Chem. Mater. 10 (1998) 72–77.
[3] H. Kato, K. Asakura, A. Kudo, J. Am. Chem. Soc. 125 (2003) 3082–3089.
[4] A. Kudo, Int. J. Hydrogen Energy 31 (2006) 197–202.
[5] K. Sayama, K. Mukasa, R. Abe, Y. Abe, H. Arakawa, Chem. Commun. 26 (2001) 2416–2417.
[6] K. Sayama, K. Mukasa, R. Abe, Y. Abe, H. Arakawa, J. Photochem. Photobiol. A: Chem. 148 (2002) 71–77.
[7] R. Abe, T. Takata, H. Sugihara, K. Domen, Chem. Commun. 30 (2005) 3829–3831.
[8] A. Kudo, K. Omori, H. Kato, J. Am. Chem. Soc. 121 (1999) 11459–11467.
[9] H. Kato, H. Kobayashi, A. Kudo, J. Phys. Chem. B 106 (2002) 12441–12447.
[10] J.A. Nozik, Phys. Rev. B 6 (1972) 453–459.
[11] T. Yiwen, J. Yun, J. Zhiyong, L. Bihui, L. Lijuan, X. Liang, Inorg. Chem. 45 (2006) 10774–10778.
[12] D.R. Kammler, T.O. Mason, K.R. Poeppelmeier, Chem. Mater. 12 (2000) 1954–1960.
[13] M.C. Payne, M.P. Teter, D.C. Alan, Rev. Mod. Phys. 64 (1992) 1045–1097.
[14] M.D. Segall, P.L.D. Lindan, M.J. Probert, J. Phys.: Condens. Matter 14 (2002) 2717–2744.
[15] M.E. Bowden, C.M. Cardile, Powder Diffr. 5 (1990) 36–40.
[16] M.A. Butle, J. Appl. Phys. 48 (1977) 1914–1920.
[17] K. Maeda, N. Saito, D. Lu, Y. Inoue, K. Domen, J. Phys. Chem. C 111 (2004) 4749–4755.